



Thermodynamic parameters of the interaction of *Urtica dioica* agglutinin with N-acetylglucosamine and its oligomers

Reiko T. Lee^{1*}, Hans-Joachim Gabius² and Yuan C. Lee¹

¹ Department of Biology, Johns Hopkins University, 3400 N. Charles Street, Baltimore, MD 21218, USA

² Institut für Physiologische Chemie, Ludwig-Maximilians-Universität, Veterinärstr. 13, D-80539 München, Germany

The interaction between *Urtica dioica* agglutinin (UDA) and N-acetylglucosamine (GlcNAc) and its $\beta(1-4)$ -linked oligomers was studied by fluorescence titration and isothermal titration microcalorimetry. UDA possesses one significant binding site that can be measured calorimetrically. This site is composed of three subsites, each subsite accommodating one GlcNAc residue. The interaction is enthalpically driven, and the binding area of UDA is characterized by a ΔH of interaction for a given oligosaccharide considerably smaller than that of wheat germ agglutinin (WGA), despite the fact that they both belong to a family of proteins composed entirely of hevein domains. Relatively high ΔC_p values of the UDA-carbohydrate interactions and more favorable entropy term compared to WGA suggest that binding of the carbohydrate ligands by UDA has a higher hydrophobic component than that of WGA.

Keywords: *Urtica dioica* agglutinin, GlcNAc-binding lectin, microcalorimetry, lectin-ligand interaction

Introduction

Lectins with a similar ligand-binding property from different organisms often have a related structural motif. In the case of chitin-binding and related proteins, a domain called hevein domain is predominantly represented with varying degrees of repeat number, or tandemly linked to other domains [1]. Hevein itself is a small, 43-amino acid residue protein (4.5 kDa) isolated from rubber tree latex that recognizes GlcNAc and its oligomers. Hevein domains are rich in cysteines and glycines, with three perfectly conserved and one slightly misaligned disulfide bonds, but these domains contain little secondary structure. Crystallographic structure of hevein as well as its solution structures based on nuclear magnetic resonance (NMR) study have been reported [2–4]. *Urtica dioica* agglutinin (UDA) (9 kDa) belongs to the hevein family having two such domains tandemly connected with a short linker [5]. Interestingly, both hevein and UDA appear to be produced as a part of larger proteins, since their cDNAs encode not only hevein domain(s) but also an unrelated domain on the C-terminal side that resembles either a chitinase domain or a wound-inducible protein domain [6, 7]. Wheat germ agglutinin (WGA), perhaps the best known member of the family, is

a homodimeric protein with each monomer composed of four hevein domains. These hevein domains are quite homologous to each other but not identical, and some domains appear to have lost the ability to bind GlcNAc and its oligomers.

We studied the interaction of UDA with GlcNAc and its oligomers by isothermal titration calorimetry (ITC) and fluorescence titration. The results suggest that there is one significant binding site per molecule of UDA, and that this binding site is composed of three subsites. The similarity and differences in the binding area architecture and thermodynamic properties between UDA and WGA are discussed.

Materials and methods

N-Acetylglucosamine (GlcNAc) was obtained from Sigma Chemical Co. (St. Louis, MO). Oligosaccharides (di- to penta-) of $\beta(1-4)$ GlcNAc linkages were from Seikagaku America (Rockville, MD) and were >99% pure. UDA was isolated from rhizomes and purified by affinity chromatography on chitin, which had been thoroughly washed with acid and base to remove an agglutinating compound [8], followed by cation exchange chromatography as described [9, 10]. Since UDA has a propensity to form higher molecular-weight complexes, a further step of gel filtration on Bio-Gel P-10 AQ was included. The UDA preparations thus obtained were characterized for their isolectin

* To whom correspondence should be addressed. Tel: 1-410-516-7322; Fax: 1-410-516-8716; E-mail: Reiko.lee@jhu.edu

pattern with a Mono-S column AQ and for their weak hemagglutinating activity using rabbit erythrocytes [11]. Concentration of UDA was determined by fluorescamine assay after alkaline hydrolysis [12] using wheat germ agglutinin (WGA, from E-Y Labs, San Mateo, CA) as standard.

Fluorescence spectra were obtained using a Perkin Elmer Luminescence Spectrometer LS 50B. Fluorometric titration was carried out in 50 mM sodium phosphate buffer, pH 7, containing 50 mM NaCl. To 3 ml of UDA solution ($\sim 20 \mu\text{g ml}^{-1}$) in a cuvette containing a small stirring bar, a ligand solution (a GlcNAc oligosaccharide) was added in 10 μl portions. After each addition, the solution was stirred well and fluorescence spectrum (310–400 nm) was taken using the excitation wavelength of 295 nm. The concentration of ligand solution added varied depending on the affinity of each ligand: e.g., for di-N-acetylchitobiose [(GlcNAc)₂], 46 mM and 140 mM solutions and for tetra-N-acetylchitotetraose [(GlcNAc)₄], 3 mM and 6 mM solutions were used. The initial segment of titration was done using the less concentrated of the two solutions. Due to its very low affinity, GlcNAc was added to UDA solution as solid. Correction for small volume changes upon addition of solid GlcNAc was done by carrying out a parallel addition of GlcNAc to an identical lectin solution.

The association constants of UDA-ligand interactions were determined from increase in fluorescence at 340 nm, using two different plots: a Scatchard plot of v/C_f versus v , and a plot of $\log(F - F_0)/(F_\infty - F)$ versus $\log C_f$ [13], where v is the fraction of liganded UDA, C_f is the concentration of free ligand, F is the observed fluorescence, and F_0 and F_∞ are fluorescence in the absence and at a saturating concentration of the ligand, respectively. F_∞ was obtained by plotting $(F - F_0)/C_f$ on y axis versus $(F - F_0)$ on x axis, and extrapolating the line to the intercept at x axis.

The isothermal titration calorimetry (ITC) was performed on a MicroCal OMEGA titration calorimeter (MicroCal Inc., Northampton, MA), using the original software provided by the company. Both UDA and GlcNAc oligomers were dissolved in the same phosphate buffer (pH 7) used in the fluorescence titration, and aliquots of GlcNAc oligomer solution were titrated into the UDA solution. For each titrant, ITC experiments were carried out at four temperatures between 15 and 35 °C. An ITC experiment was also carried out in a Tris buffer (50 mM Tris/HCl with 50 mM NaCl, pH 7) for (GlcNAc)₃. Data were analysed using the software developed at the Biocalorimetry Center (The Johns Hopkins University). Figure 4 shows representative ITC experimental data (top panel) and analysis (bottom panel), the curve being generated using program "Origin" available from MicroCal.

Results

Fluorescence titration

UDA is a small protein composed of 89 amino acid residues with five tryptophan residues. Fluorescence spectrum of

UDA shows a maximum at ~ 350 nm with a shoulder at 330 nm. The peak shifts slightly to a shorter wavelength (345 nm) upon addition of GlcNAc oligosaccharides concomitant with an increase in fluorescence intensity (Figure 1). This blue shift was not observed when GlcNAc was used as ligand. The maximum fluorescence enhancement $[(F_\infty - F_0)/F_0] \times 100$ for GlcNAc, (GlcNAc)₂, (GlcNAc)₃ and (GlcNAc)₄ was 5.3, 15.8, 27 and 26%, respectively, compared to 46% for the WGA-(GlcNAc)₃ interaction [13].

When the data were analyzed by Scatchard plot, (GlcNAc)₃ and (GlcNAc)₄ gave curved lines as seen in Figure 2, whereas GlcNAc and (GlcNAc)₂ gave straight lines. For the curved lines, two K_a values were estimated from the upper and the lower segment of the curve. Plots of $\log(F - F_0)/(F_\infty - F)$ versus $\log C_f$ for all four ligands are shown in Figure 3. K_a values obtained from the slope of Scatchard plots and from the double logarithmic plots (at $y = 0$) are presented in Table 1.

Isothermal titration

The ITC experiments in which $\beta(1-4)$ -linked GlcNAc oligosaccharides were titrated into UDA solution all produced titration curves similar to that shown in Figure 4. All

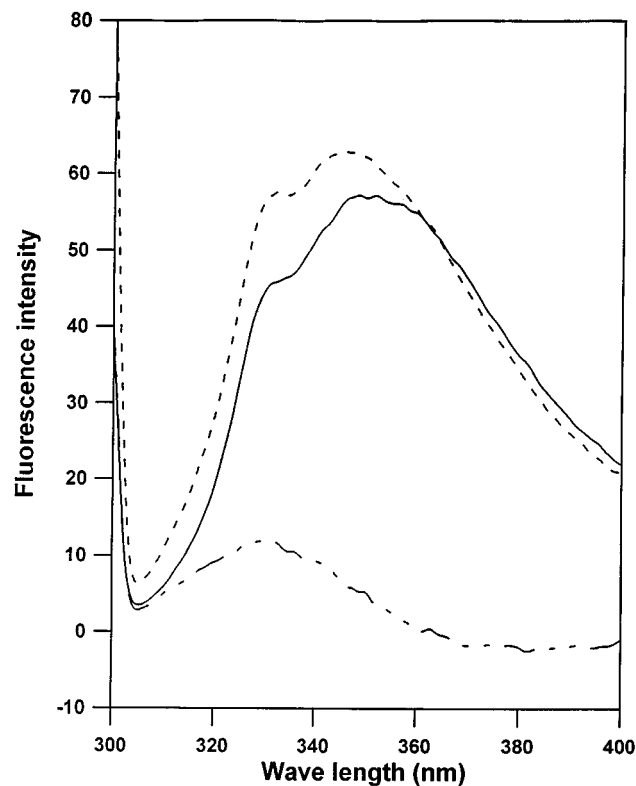


Figure 1. Fluorescence emission spectra of UDA. Solid line, UDA alone; dashed line, UDA in the presence of 0.84 mM (GlcNAc)₃; uneven dashed line, difference spectrum.

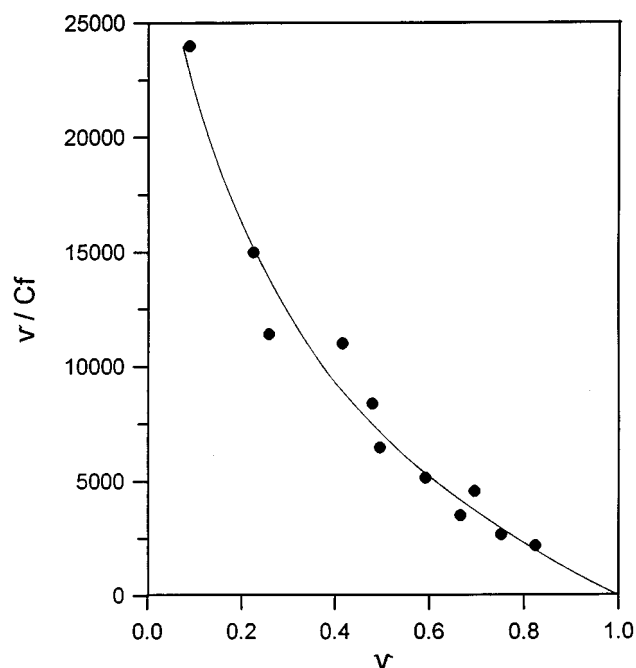


Figure 2. A typical Scatchard plot of fluorescence titration data. Interaction of UDA with (GlcNAc)₄. v , fraction of sites occupied by ligand; C_f , concentration of free ligand.

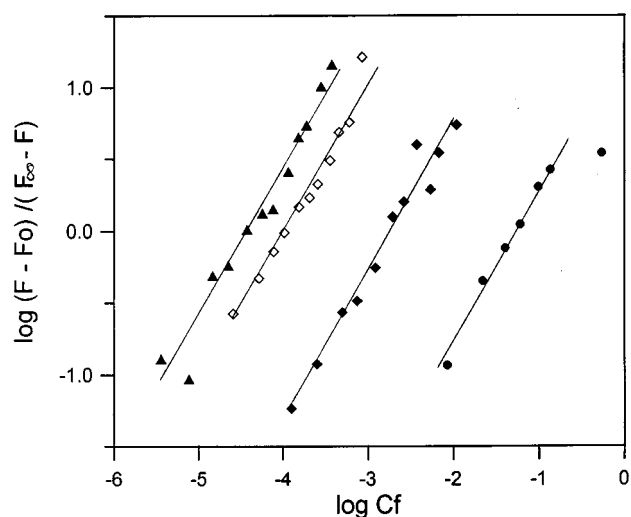


Figure 3. Plots of $\log (F - F_0) / (F_\infty - F)$ versus $\log C_f$, where F , F_0 and F_∞ are observed fluorescence, fluorescence without ligand, and fluorescence at saturating concentration of ligand. Ligands used are: ●, GlcNAc; ◆, (GlcNAc)₂; ◇, (GlcNAc)₃; ▲, (GlcNAc)₄.

the titration curves reached plateau at the highest ligand concentration, indicating the saturation of the binding sites. Data were fit with constraints of n (number of binding sites per molecule) = 1 and $n = 2$. For $n = 2$, the affinity of the two sites was either allowed to be dissimilar or constrained to the same value. Standard deviation (ssr) was generally

Table 1. Association constant of the UDA interaction with GlcNAc and its oligosaccharides obtained from fluorescence titration

	$K_a \times 10^{-3}$		
	from Scatchard plot		from Double-log plot
GlcNAc	0.02		0.017
(GlcNAc) ₂	0.48		0.48
(GlcNAc) ₃	11.6	4.2	7.1
(GlcNAc) ₄	58	16	25

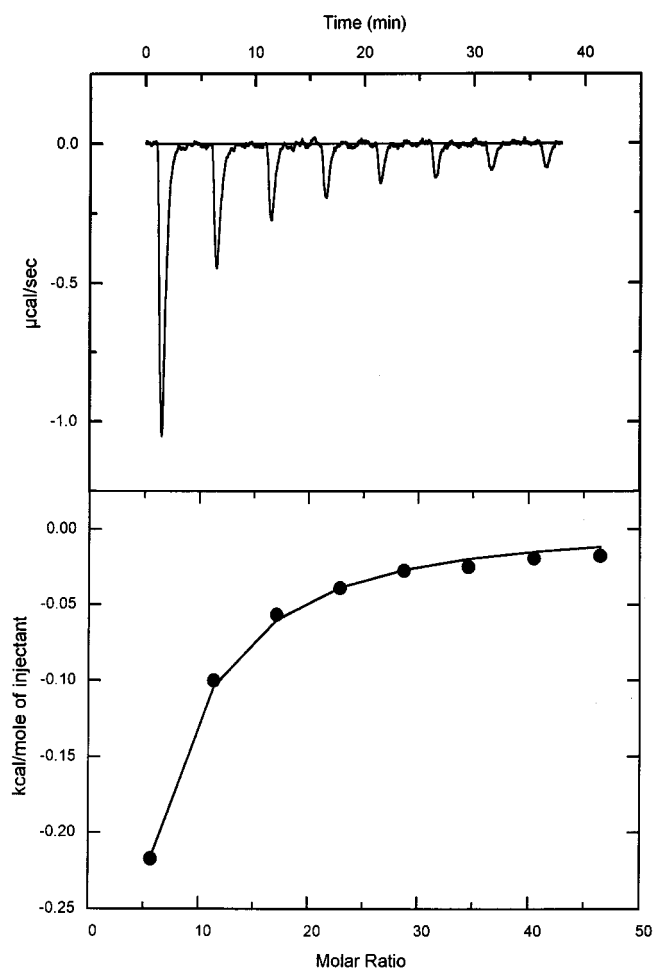


Figure 4. A typical ITC data and analysis: top panel, heat produced by injecting (GlcNAc)₃ solution to UDA solution; bottom panel, titration curve of cumulative heat produced plotted against the total amount of the ligand added. Although the data were analyzed by the software developed in Biocalorimetry Center, The Johns Hopkins University, this figure was generated using program "Origin" available from MicroCal.

smaller for the $n = 1$ fitting than for the $n = 2$ fitting with $K_{a1} = K_{a2}$. Fitting with $n = 2$ of dissimilar K_a improved ssr only slightly over the $n = 1$ fitting. However, this

Table 2. A comparison of thermodynamic parameters for WGA and UDA

Ligand	WGA ^a				UDA				
	$-\Delta H$ kcal/mol	$-T\Delta S$ kcal/mol	$-\Delta G$ kcal/mol	$K_a \times 10^{-3}$	$-\Delta H$ kcal/mol	$-T\Delta S$ kcal/mol	$-\Delta G$ kcal/mol	$K_a \times 10^{-3}$	$K_a \times 10^{-3}$
GlcNAc	6.1	2.4	3.7	0.41					0.017
(GlcNAc) ₂	15.6	10.5	5.1	5.3	4.7	0.8	3.9	0.8	0.48
(GlcNAc) ₃	19.4	13.9	5.5	11.1	6.3	1.2	5.1	6.2	7.1
(GlcNAc) ₃ ^c					8.6	3.4	5.2	6.2	
(GlcNAc) ₄	19.2	13.6	5.6	12.3	5.1	-0.5	5.6	14.4	25
(GlcNAc) ₅	18.2	12.4	5.8	19.1	5.1	-0.8	5.9	26.5	

^a Thermodynamic data are from Baines G *et al.* [14].

^b K_a values from fluorescence determinations.

^c Titration data were obtained for this interaction in a tris-HCl buffer, pH 7.0, instead of the phosphate buffer.

improvement in the quality of the fit corresponds to what is expected by an increase in the number of fitting parameters. For this reason and for reasons presented in Discussion, the number of functional binding sites in UDA is likely to be one.

Thermodynamic parameters of UDA interaction with four GlcNAc oligosaccharides obtained with the $n = 1$ fitting are summarized in Table 2. For comparison, K_a values obtained from fluorescence titration and calorimetric data for WGA [14] are also included in the same table. The table shows that K_a values obtained by fluorescence and calorimetry agreed quite well. Generally the values of $-\Delta G$ were similar or smaller than the corresponding values of $-\Delta H$, indicating that the UDA-carbohydrate interaction is enthalpically driven, as was generally found for lectin-carbohydrate interactions [15]. Data for the UDA interaction with (GlcNAc)₃ in phosphate and tris buffers were similar, suggesting that there is no net proton transfer during the binding. For each ligand, the ΔC_p value was obtained from the slope of the plot of ΔH vs T . The ΔC_p values were $-153 \text{ cal K}^{-1} \text{ mol}^{-1}$ for (GlcNAc)₂, $-125 \text{ cal K}^{-1} \text{ mol}^{-1}$ for (GlcNAc)₃, $-114 \text{ cal K}^{-1} \text{ mol}^{-1}$ for (GlcNAc)₄ and $-121 \text{ cal K}^{-1} \text{ mol}^{-1}$ for (GlcNAc)₅.

Discussion

The hevein domain (43 amino acid residues) is a small, GlcNAc-recognizing domain that is abundantly represented in the plant kingdom in the form of basic chitinases and chitin-binding proteins. Hevein itself is capable of binding GlcNAc and its oligomers as shown by the NMR study [4]. UDA, from rhizome of stinging nettle, is composed of two hevein domains tandemly conjoined, and it is reported to exist as a monomer [9]. WGA, on the other hand, is a much larger protein of the hevein family. It exists as homodimer with each monomeric unit composed of four tandemly joined hevein domains, designated as domain A, B, C, and

D from the N-terminal end [16]. The X-ray crystallographic study showed that the monomeric unit exists in a disc-like form and that two such discs (monomers) associate to form a sandwich-like structure, with A domain of one monomer apposing D domain of the other, and B domain of one apposing C domain of the other. The ligand-binding sites of WGA are located in the interface between the two monomers [16]. Specifically, the primary binding sites are located between B and C domains belonging to different monomeric units, and the secondary binding sites between A and D domains, again belonging to different monomeric units. Thus, there are four binding sites per WGA molecule, although there are eight hevein domains. The primary and the secondary binding sites actually exhibit very similar saccharide binding mode, despite the fact that they are constituted of different domains. For both types of binding site, both hydrogen bond and van der Waals interactions are important in the ligand binding. Although two domains participate in the binding at each binding site, the majority of the contributing side chains and backbones of amino acid residues are located on one of the domains [16].

Table 2 shows that $-\Delta H$ of WGA for each ligand is more than 3-fold larger than the corresponding $-\Delta H$ for UDA. However, the larger enthalpy of interaction for WGA compared to UDA is significantly compensated by an unfavorable entropy term, so that $-\Delta G$ for a particular ligand, e.g. (GlcNAc)₂, is only modestly larger for WGA than for UDA. A large disparity in both ΔH and ΔS between the two lectins suggests a considerable difference in the binding mode of the two lectins. Since UDA exists as monomer and its two domains are connected by a short peptide piece of only four amino acid residues, it is unlikely that the UDA domains can appose each other to form an interface similar to that found in the dimeric WGA molecule. Therefore, the binding area of UDA is probably similar to hevein and is more exposed to bulk solvent than that of WGA. The solvent-exposed binding area of UDA is expected to

produce smaller enthalpy of interaction than the WGA binding area, which being at the interface of two apposing protein domains would likely interact with a larger protein surface area.

Table 2 shows that the entropy term of UDA-carbohydrate interactions is much more favorable than the corresponding WGA entropy term, and ΔS of some UDA-carbohydrate interactions in fact takes positive values. Most lectin-carbohydrate interactions exhibit small, negative ΔS values, although positive ΔS values have been reported [15]. ΔC_p values for UDA-carbohydrate interactions range between $-100 \text{ cal K}^{-1} \text{ mol}^{-1}$ and $-150 \text{ cal K}^{-1} \text{ mol}^{-1}$, and their absolute values, although small, lie on the high side of the most lectin-carbohydrate interactions. In most lectin-carbohydrate interactions, the ΔC_p term appears to reflect mainly changes in the solvent organization accompanying the binding process, and a larger ΔC_p term suggests a more hydrophobic nature of the binding area [15]. These facts suggest that unliganded UDA may have a significant area of exposed hydrophobic surface in or near the GlcNAc-binding site, and the binding of GlcNAc oligosaccharides can help bury those surfaces from the solvent.

The binding of GlcNAc and $(\text{GlcNAc})_2$ by hevein studied by NMR identified the area of interaction to be located between amino acid residues 19 to 30 [4] (Figure 5). This area contains three aromatic amino acids (Trp21, Trp23 and Tyr30), and these residues as well as Ser19 seem to participate in the interaction with sugar. Both Trp21 and Trp23 in hevein appear to be solvent-exposed, as verified by different NMR techniques [4, 17]. Inspection of UDA sequence [5] reveals that these four amino acids are conserved at the exact location in the first domain of UDA, but in the second domain one of the Trp moieties (one corresponding to Trp21) is replaced by His. A study of UDA- $(\text{GlcNAc})_3$ interaction by NMR [18] indeed identified a peptide segment containing Trp21 and Trp23 as well as Tyr30 of the first hevein domain of UDA to be the primary site of interaction.

The binding of GlcNAc oligosaccharides by UDA causes its fluorescence to increase at $\sim 340 \text{ nm}$ with an accompanying blue shift, suggesting that some solvent-exposed

tryptophan residues in UDA become shielded from solvent by the ligand. The maximal fluorescence enhancement attained upon binding of a ligand is rather small but increases with increasing ligand size up to the trisaccharide (5.3% for GlcNAc to 27% for the trisaccharide). Since there are five Trp residues in UDA, the low degrees of fluorescence enhancement may mean that at most two Trp residues become more shielded from solvent when a ligand is bound. It is tempting to postulate that the two Trp residues implicated in the fluorescence study are Trp21 and Trp23 of the first domain. Notably, the ligand binding is accompanied by a change in the appearance of Trp21 and Trp23 signals in CIDNP (chemically induced dynamic nuclear polarization) spectra, indicating an altered dye accessibility to Trp21 upon binding of $(\text{GlcNAc})_4$ [17]. WGA on the other hand produced the maximal fluorescence enhancement of 46% [13]. Although the reported Trp content was four residues per monomer, the actual content based on cDNA sequencing is found to be three Trp residues per monomer [19]. The difference in the maximal fluorescence enhancement between UDA and WGA is in line with the observations in the CIDNP study that showed the change in CIDNP signals in the presence of dye to be considerably larger for WGA than for UDA [17]. Interestingly, for both WGA and UDA, the binding of GlcNAc caused much smaller fluorescence enhancement and this increase was not accompanied by a shift in the maximum wavelength.

Ligand-binding studies by equilibrium dialysis [20] suggested that UDA has two binding areas of dissimilar affinity, and the affinity of the stronger site determined by hapten inhibition assay agreed reasonably with our results. The NMR study of UDA- $(\text{GlcNAc})_3$ interaction [18] also identified the second binding site with more than ten fold lower affinity, which is located in the second hevein domain of UDA. In our fluorescent study, we observed moderate curvature in the Scatchard plots of the fluorescence titration data when larger GlcNAc oligosaccharides were used. If this is interpreted to mean the presence of two binding sites of dissimilar affinity on UDA, the affinity difference is only about 3–3.5 fold (Table 1), much smaller than that reported in the literature. On the other hand, all of our isothermal

Hevein	EQCGRQAGGK ¹⁰ LCPNNLCCSQ ²⁰ GWGCGSTDEY ³⁰ CSPDHNCQSN ⁴⁰ CKD
WGA-1 domain C	IK--S----- --F--LGS-F -GGGCQSGAC ST-
UDA domain 1	QR--S-G--G T--ALW---I -----DSEP- -GRTCENKCW SGERSD
UDA domain 2	HR--AAV-NP P-GQDR---V H----GGND- --GSKCQYRC SSS

Figure 5. Amino acid sequence alignment of some hevein domains. –, residue identical to the corresponding amino acid of hevein.

titration curves (e.g., Figure 4) reached plateau with no suggestion of significant upward drift at higher ligand concentrations. Although the SSR values were similar or slightly smaller when the number of sites (n) was set at two with no restriction on K_a , the fitting actually improved only at the first point on the titration curve and produced a second site of even higher affinity than the first site (5 to 1000-fold) with an unfavorable ΔH or a ΔH much smaller than the first site. For these reasons, we believe our calorimetry data fit best to a one-site model and suggest the presence of one binding site on the UDA molecule that can be measured calorimetrically. The fact that we did not observe a binding site of much lower affinity in our calorimetric study is not surprising, because, in addition to the concentrations of reactants used being not high enough to saturate such a site, ΔH values at this site would be expected to be considerably smaller than at the first site even at saturation.

Affinity of UDA toward GlcNAc and its oligomers increases substantially with each added GlcNAc residue up to trisaccharide, and continues to increase gradually with additional GlcNAc units (Table 2). This interaction between UDA and the fourth and fifth GlcNAc residues is quite small and does not involve an increase in enthalpy. Therefore, it appears that UDA possesses three subsites at its binding area, each subsite having lower intrinsic affinity than the preceding subsite. That the binding area consists of three subsites was also proposed by Shibuya *et al.* [20]. The number of subsites is the same as proposed for WGA [13, 14, 21], which is reasonable in view of the homology

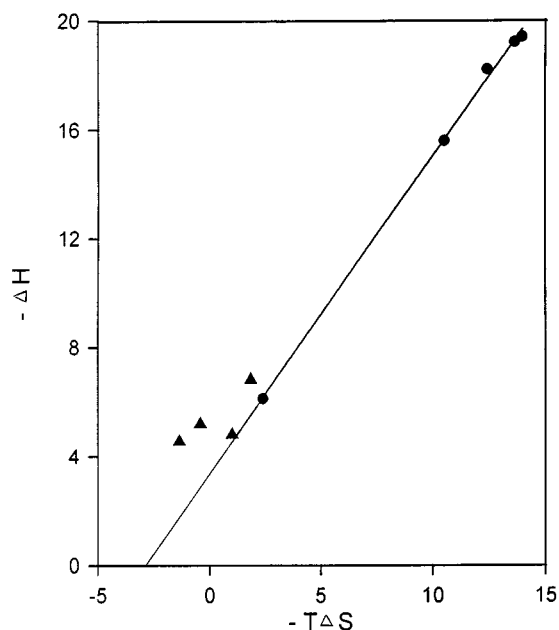


Figure 6. Plot of $-\Delta H$ versus $-T\Delta S$; ●, interaction of WGA with $(\text{GlcNAc})_n$, where $n = 1$ to 5. ▲, interaction of UDA with $(\text{GlcNAc})_n$, where $n = 2$ to 5.

shared among hevein domains. A gradual upward drift of affinity beyond trisaccharide suggests that UDA is interacting in some way with the fourth and the fifth GlcNAc residues. This interaction with the peripheral GlcNAc residues appears to be driven mainly from a favorable entropy term. A plot of ΔH versus $T\Delta S$ for the association of WGA with GlcNAc and its oligomers [14] yielded a straight line (Figure 6). This phenomenon, known as enthalpy-entropy compensation, is observed in many association processes including lectin-carbohydrate interaction that proceed in aqueous solutions. With respect to lectin-carbohydrate interaction, the more unfavorable entropy accompanying stronger enthalpy of interaction is thought to result from the reorganization of water molecules [22, 23], and/or greater restriction of mobility for the ligand [24] during the binding process. When the UDA data are also plotted in Figure 6, only the data for UDA- $(\text{GlcNAc})_2$ interaction lie on the WGA line, while the data for larger oligosaccharides lie above this line. Such results suggest that perhaps the nature of interaction between UDA and the first two GlcNAc residues resembles that of the WGA-ligand interactions, whereas the interaction of UDA with peripheral GlcNAc residues is more of non-specific hydrophobic nature.

Acknowledgment

We thank Dr. M.M. Lopez and Ms. M. Kasimova for obtaining and processing ITC data, and Dr. E. Freire for his generous support. This work was performed in part at the Biocalorimetry Center, a Biomedical Research Technology Resource Center sponsored by the National Institute of Health (RR04328), The Johns Hopkins University, Department of Biology, Baltimore, MD 21218, USA. We also thank J. Koopmann for helpful assistance in the early stages of establishing the lectin purification, and VW Foundation for generous financial support.

References

- Beintema JJ (1994) *FEBS Lett* **350**: 159–63.
- Rodriguez-Romero A, Ravichandran KG, Soriano-Garcia M (1991) *FEBS Lett* **291**: 307–9.
- Andersen NH, Cao B, Rodriguez-Romero A, Arreguin B (1993) *Biochemistry* **32**: 1407–22.
- Asensio JL, Canada FJ, Bruix M, Rodriguez-Romero A, Jimenez-Barbero J (1995) *Eur J Biochem* **230**: 621–33.
- Beintema JJ, Peumans WJ (1992) *FEBS Lett* **299**: 131–4.
- Lerner DR, Raikhel NV (1992) *J Biol Chem* **267**: 11085–91.
- Broekaert W, Lee H-I, Kush A, Chua N-H, Raikhel N (1990) *Proc Natl Acad Sci USA* **87**: 7633–7.
- Whitmore FW (1992) *Biotechniques* **12**: 202–8.
- Peumans WJ, De Ley M, Broekaert WF (1984) *FEBS Lett* **177**: 99–103.
- Kayser K, Bubenzer J, Kayser G, Eichhorn S, Zemlyanukhina TV, Bovin NV, André S, Koopmann J, Gabius H-J (1995) *Analyt Quant Cytol Histol* **17**: 135–42.

- 11 Van Damme EJM, Broekaert WF, Peumans WJ (1988) *Plant Physiol* **86**: 598–601.
- 12 Stowell CP, Kuhlenschmidt TB, Hoppe CA (1978) *Anal Biochem* **85**: 572–80.
- 13 Privat JP, Delmotte F, Mialonier G, Bouchard P, Monsigny M (1974) *Eur J Biochem* **47**: 5–14.
- 14 Bains G, Lee RT, Lee YC, Freire E (1992) *Biochemistry* **31**: 12624–8.
- 15 Toone EJ (1994) *Curr Opin Struct Biol* **4**: 719–28.
- 16 Wright CS (1980) *J Mol Biol* **141**: 267–91.
- 17 Siebert H-C, von der Lieth C-W, Kaptein R, Beintema JJ, Dijkstra K, van Nuland N, Soedjanaatmadja UMS, Rice A, Vliegthart JFG, Wright CS, Gabius H-J (1997) *Proteins* **28**: 268–84.
- 18 Hom K, Gochin M, Peumans WJ, Shine N (1995) *FEBS Lett* **361**: 157–61.
- 19 Wright CS, Raikhel N (1989) *J Mol Evol* **28**: 327–36.
- 20 Shibuya N, Goldstein IJ, Shafer JA, Peumans WJ, Broekaert WF (1986) *Arch Biochem Biophys* **249**: 215–24.
- 21 Allen AK, Neuberger A, Sharon N (1973) *Biochem J* **131**: 155–62.
- 22 Lemieux RU, Delbaere LTJ, Beierbeck H, Spohr U (1991) *Ciba Found Symp* **158**: 231–48.
- 23 Siebert H-C, von der Lieth C-W, Gilleron M, Reuter G, Wittmann J, Vliegthart JFG, Gabius H-J (1997) in *Glycosciences: Status and Perspectives* (Gabius H-J, Gabius S, eds) pp 291–310, Weinheim: Chapman & Hall.
- 24 Carver JP, Michnick SW, Imberty A, Cumming DA (1989) *Ciba Found Symp* **145**: 6–26.

Received 27 October 1997, revised 9 January 1998, accepted 27 January 1998